

Application of Artificial Neural Networks in Predicting Malignant Lung Nodules on Chest CT Scans

Wenhui Li, Yuping Yang*, Yixian Liang, Pengliang Xu, Qiuqiang Chen

Department of Thoracic Surgery, Huzhou First People's Hospital, Huzhou 313000, Zhejiang Province, China

*Corresponding author: Yuping Yang, 13819281694@163.com

Copyright: © 2025 Author(s). This is an open-access article distributed under the terms of the Creative Commons Attribution License (CC BY 4.0), permitting distribution and reproduction in any medium, provided the original work is cited.

Abstract: *Objective:* To explore a simple method for improving the diagnostic accuracy of malignant lung nodules based on imaging features of lung nodules. *Methods:* A retrospective analysis was conducted on the imaging data of 114 patients who underwent lung nodule surgery in the Thoracic Surgery Department of the First People's Hospital of Huzhou from June to September 2024. Imaging features of lung nodules were summarized and trained using a BP neural network. *Results:* Training with the BP neural network increased the diagnostic accuracy for distinguishing between benign and malignant lung nodules based on imaging features from 84.2% (manual assessment) to 94.1%. *Conclusion:* Training with the BP neural network significantly improves the diagnostic accuracy of lung nodule malignancy based solely on imaging features.

Keywords: Lung nodule; Malignant lung tumor; Neural network; Chest CT

Online publication: February 13, 2025

1. Introduction

Lung cancer, as a cancer type with an increasing incidence rate^[1], poses severe consequences and high mortality if not treated promptly^[2]. Early screening and treatment are therefore of great significance^[3]. Chest CT, as the most important examination for detecting lung nodules^[4], has been widely implemented as part of routine physical check-ups in recent years. However, lung nodules identified on chest CT can be either benign or malignant. Benign solitary lung nodules are often granulomatous lesions or hamartomas. Unless the nodules are large and cause compression symptoms, surgical treatment of such benign nodules does not benefit patients. Therefore, in addition to detecting lung nodules, distinguishing between benign and malignant nodules is a critical aspect of chest CT interpretation^[5].

This study aims to assess the lung cancer positivity rate among surgical lung nodule cases handled in our department and to summarize a straightforward machine-learning-assisted diagnostic method suitable for clinical application.

2. Materials and methods

This study was approved by the Ethics Committee of the First People's Hospital of Huzhou. It included 114 patients who underwent lung nodule surgery at the hospital from June to September 2024.

Inclusion criteria: (1) Completion of preoperative chest CT examination at this hospital; (2) Clear pathological diagnosis after surgery.

Exclusion criteria: (1) Resection of small, non-primary lesions; (2) Unclear pathological diagnosis after surgery.

Chest CT interpretation and data collection were independently completed by three thoracic surgeons from the research team. The final data was confirmed after verifying the consistency of the results. The imaging features of lung nodules, including lobulation, spiculation, burr sign, pleural indentation, vacuole sign, and ground-glass opacity (**Figure 1**), were recorded. Positive features were recorded as 1, and negative features as 0. Pathological results were recorded as 1 for malignant and 0 for benign.

General information such as the gender and age of the surgical patients was compiled, and the proportion of malignant nodules among the surgical cases was recorded. The proportions of ground-glass opacity, burr sign, spiculation, vacuole sign, lobulation, and pleural indentation were calculated and compared between benign and malignant groups.

Statistical methods: χ^2 tests were used for statistical analysis, performed using SPSS 21.0 software.

Neural network algorithm: A Back Propagation (BP) neural network was selected for analysis. Its architecture includes an input layer, a hidden layer, and an output layer.

- (1) The input layer consisted of six neurons, corresponding to six imaging features of lung nodules from chest CT scans.
- (2) The hidden layer contained seven neurons, chosen based on MATLAB's official recommendations.
- (3) The output layer consisted of two neurons, corresponding to benign or malignant nodules (**Figure 2**).

The dataset was divided into training, validation, and testing sets, with proportions of 70%, 15%, and 15%, respectively. The training was performed using the conjugate gradient algorithm. The entire training process was conducted using MATLAB 2022b software.

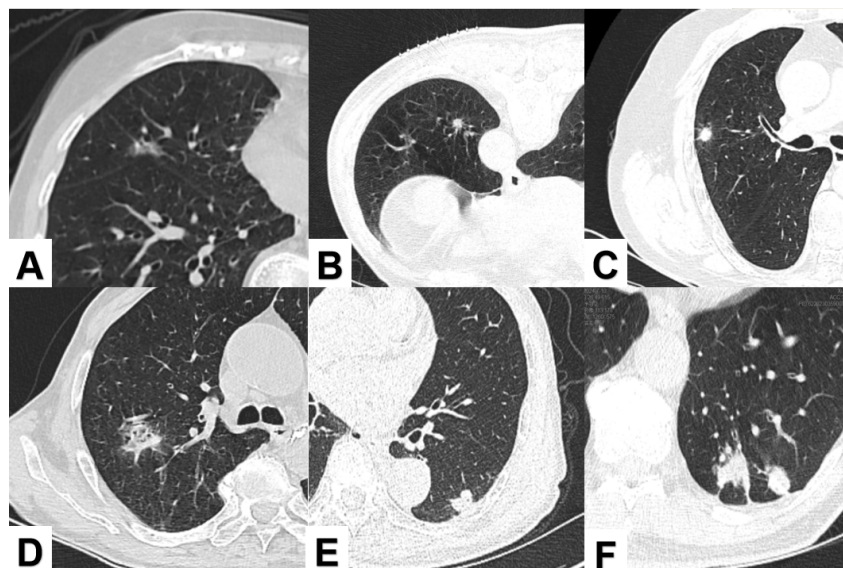


Figure 1. (A) Ground-glass opacity; (B) Burr sign; (C) Spiculation; (D) Vacuole sign; (E) Lobulation; (F) Pleural indentation

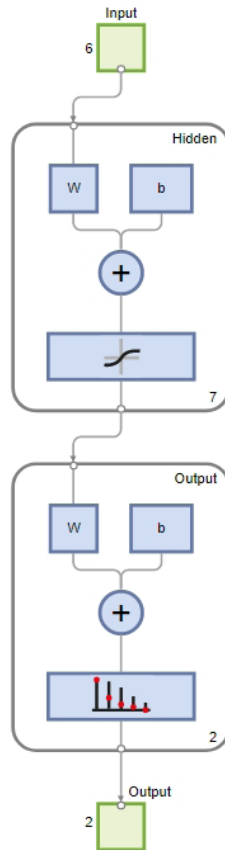


Figure 2. The BP neural network consists of three layers: input, hidden, and output. The data flows from the input layer to the hidden layer, where it is multiplied by weights (w) and added to biases (b), then passed through a sigmoid function to the output layer. Similarly, in the output layer, the data undergoes multiplication by weights and the addition of biases before being passed through a sigmoid function. The squared error between the output value and the expected value is back-propagated to calculate the partial derivatives of weights for each neuron, which are adjusted accordingly. The network learning ends when the error reaches the expected value.

3. Results

3.1. Basic information

Among the 114 patients included, 47 were male (42.23%), and 67 were female (57.77%), with an average age of 64.25 ± 12.21 years. Postoperative pathological results showed 96 cases of malignancy (84.21% of the total) and 18 cases of benign lesions (**Table 1**).

Among the cases, ground-glass opacity, burr sign, spiculation, vacuole sign, lobulation, and pleural indentation were observed in 79.17%, 62.50%, 70.83%, 28.13%, 65.63%, and 28.13% of patients, respectively. For patients with benign nodules, these features appeared at rates of 16.67%, 33.33%, 55.56%, 55.56%, 27.78%, and 22.22%, respectively. A comparison between the two groups showed that ground-glass opacity, burr sign, spiculation, vacuole sign, and lobulation were more frequently observed in patients with lung cancer, with statistical significance ($P < 0.05$). Although pleural indentation was more common in malignant cases, the difference was not statistically significant ($P = 0.609$, **Table 2**). This may be because many lung nodules, whether malignant or benign, were not located near the pleural surface, which limited the manifestation of pleural

indentation. Subgroup analysis focusing on nodules on the pleural surface revealed that malignant nodules were significantly more likely to exhibit pleural indentation than benign ones ($P < 0.05$, **Table 3**).

Table 1. Gender, age, and proportion of malignant nodules in 114 patients

Gender		Age (years)	Postoperative pathology	
Male	Female		Malignant	Benign
47 (42.23%)	67 (57.77%)	64.25 ± 12.21	96 (84.21%)	18 (15.79%)

Table 2. Proportions of imaging features in 114 patients and comparison between malignant and benign groups

Feature	Malignant		Benign		P value
	n	%	n	%	
Ground-glass	76	79.17%	3	16.67%	2.32E-08
Burr sign	60	62.50%	6	33.33%	0.021
Spiculation	68	70.83%	1	55.56%	3.93E-08
Vacuole	27	28.13%	1	55.56%	0.0416
Lobulation	63	65.63%	5	27.78%	0.002
Pleural indentation	27	28.13%	4	22.22%	0.609

Table 3. Comparison of pleural surface nodules with pleural indentation in malignant and benign groups

Item	Malignant		Benign		P value
	n	%	n	%	
Pleural indentation	27/35	87.10%	4/9	44.44%	0.038

3.2. Neural network training results

Cross-entropy, a measure of the difference between two probability distributions, was used to evaluate the predictive model's deviation from actual results. In the training, validation, and testing sets, the cross-entropy values were 0.0375, 0.0588, and 0.0375, respectively, indicating high agreement between the predictive model and actual data (**Table 4**).

The BP neural network achieved a diagnostic accuracy of 96.2% for malignant lung nodules in the training set, 100% in the validation set, and 94.1% in the testing set (**Table 5**).

Table 4. Cross-entropy and error values for neural network training

	Observation	Cross-entropy	Error value
Training	80	0.0765	0.0375
Validation	17	0.0239	0.0588
Testing	17	0.1193	0.0375

Table 5. Confusion matrices of BP neural network training results

Training confusion matrix				Validation confusion matrix					
Output class	1	66	2	97.1%	Output class	1	15	0	100%
		82.5%	2.5%	2.9%			88.2%	0.0%	0.0%
	2	1	11	91.7%		2	0	2	100%
		1.2%	13.8%	8.3%			0.0%	11.8%	0.0%
		98.5%	84.6%	96.2%			100%	100%	100%
		1.5%	15.4%	3.7%			0.0%	0.0%	0.0%
	1	2		1	2				
	Target class				Target class				

Testing confusion matrix				Cumulative confusion matrix					
Output class	1	14	1	93.3%	Output class	1	95	3	96.9%
		82.4%	5.9%	6.7%			83.3%	2.6%	3.1%
	2	0	2	100%		2	1	15	93.8%
		0.0%	11.8%	0.0%			0.9%	13.2%	6.2%
		100%	66.7%	94.1%			99.0%	83.3%	96.5%
		0.0%	33.3%	5.9%			1.0%	16.7%	3.5%
	1	2		1	2				
	Target class				Target class				

4. Discussion

Interpreting lung nodule imaging is undoubtedly a fundamental skill for thoracic surgeons, who are directly responsible for determining the surgical indications for lung nodules. Most lung nodule surgeries aim to address malignancy concerns and proceed with radical lung cancer surgery. Thoracic surgeons assess the benign or malignant nature of lung nodules primarily through chest CT imaging, focusing on reading the radiographic characteristics of the nodules [6]. These include lobulation, spiculation, burr sign, pleural indentation, air bronchogram, calcification, ground-glass opacity, solid components, and mixed features, among others [7]. While individual imaging features may have statistical significance in predicting malignancy, they are insufficient for definitive characterization. Determining malignancy requires a combination of multiple features, which introduces ambiguity and inevitably leads to misdiagnosis or missed diagnoses [8]. In this study, the positive rate of lung cancer among surgical patients with lung nodules was only 84.2%. This indicates room for improvement, and the identification of malignant lung nodules requires additional diagnostic tools.

Artificial intelligence (AI) aims to mimic human thought processes [8], performing specific tasks via computer systems to enhance its performance. AI has been widely applied in areas such as image recognition and natural language processing. Its general principle involves setting a loss function, where the loss minimizes when a specific target is reached and increases otherwise. Among these algorithms, gradient descent (GD), particularly the back-propagation algorithm (BP), is widely used. The basic principle involves inputting information through the input layer, processing it in the hidden layer, and outputting it via the output layer. The output is then compared

with the expected value. If the error is large, it propagates back to the hidden layer, where weights in the data transmission process are purposefully adjusted based on the magnitude and direction of the error. Ultimately, this process brings the output closer to the expected value. In medical subspecialties supported by large datasets, machine learning has naturally found a significant role. For instance, in pathology, machine learning has been used to analyze large volumes of pathological slides to diagnose gastric cancer^[9,10], lung cancer^[11], renal cancer^[12], prostate cancer^[13], and hypopharyngeal squamous cell carcinoma^[14]. Similarly, imaging has improved diagnostic accuracy for breast cancer^[15], liver cancer^[16], gallbladder cancer^[17], and pituitary tumors^[18] using CT imaging.

Currently, AI-based chest CT interpretation for screening lung nodules and distinguishing between benign and malignant lesions has been applied clinically^[19]. However, its use comes at a significant cost and is mostly limited to large hospitals. Even in cases where AI is used for imaging in radiology departments, it is rarely extended to thoracic surgeons. Moreover, many radiologists do not make definitive judgments about the benign or malignant nature of lung nodules in chest CT reports, leaving the decision to thoracic surgeons. As mentioned earlier, most lung nodule surgeries are managed by attending surgeons or above, yet the positive rate for lung cancer remains only 84.2%. Therefore, simple AI-assisted diagnostic tools hold significant potential value for thoracic surgeons.

To balance simplicity and accuracy, we focused exclusively on chest CT nodule features without considering patient characteristics such as gender and age, as their association with malignant lung nodules is relatively weak. Among lung nodule-related features, we studied only those closely related to distinguishing between benign and malignant nodules, such as burr signs, spiculation, and pleural traction. In this study, the discrimination accuracy for malignant lung nodules exceeded 94% across the training, validation, and test groups while requiring only six imaging features. This achieved a favorable balance between simplicity and accuracy.

Funding

Zhejiang Medical and Health Technology Project (Project No. 2020PY072)

Disclosure statement

The authors declare no conflict of interest.

References

- [1] Zhang J, 2023, Research on Semantic Segmentation Algorithm for Pulmonary Nodules Based on 3D U-Net, dissertation, Northwest A&F University.
- [2] Pei Q, Luo Y, Chen Y, et al., 2022, Artificial Intelligence in Clinical Applications for Lung Cancer: Diagnosis, Treatment and Prognosis. *Clin Chem Lab Med*, 60(12): 1974–1983. <https://doi.org/10.1515/cclm-2022-0291>
- [3] Yang X, Zhou Y, Chen F, et al., 2024, Construction and Practice of a Comprehensive Management Model for Pulmonary Nodules/Lung Cancer Based on “Internet+”. *West China Medical Journal*, 39(4): 613–618.
- [4] Chen Q, Zhu Q, Gu J, et al., 2023, Comparative Value of HRCT Targeted Scanning with Physiological Ventilation Assistance and Thin-Section CT Reconstruction in Diagnosing Pulmonary Ground-Glass Nodules. *Chinese Journal of Medical Computer Imaging*, 29(1): 26–31.
- [5] Zhao S, Meng L, Guo J, 2022, Construction of a Multimodal Combined Model Nomogram Based on CT Targeted Scanning for Evaluating Solitary Pulmonary Nodules. *Radiologic Practice*, 37(10): 6.

- [6] Feng X, Zhang M, Wu B, et al., 2020, Application Value of High-Resolution CT Combined with Serum CEA and NSE in Differential Diagnosis of Benign and Malignant Solitary Pulmonary Nodules. *Chinese Journal of CT and MRI*, 18(6): 3.
- [7] Liu J, Qian W, Li L, et al., 2024, Diagnostic Value of Imaging Features and Quantitative Parameters in Differentiating Benign and Malignant Pulmonary Nodules. *Chinese Medical Engineering*, 32(3): 25–30.
- [8] Fu Y, Xue P, Xiao T, et al., 2023, Semi-Supervised Adversarial Learning for Improving the Diagnosis of Pulmonary Nodules. *IEEE J Biomed Health Inform*, 27(1): 109–120. <https://doi.org/10.1109/JBHI.2022.3216446>
- [9] Li J, Song Z, Chen W, et al., 2024, Discussion on the Impact of Different Staining Modes on AI Diagnosis of Gastroscopy Tissue Pathology. *Journal of Diagnostic Pathology*, 31(9): 910–912.
- [10] Zhang J, Song Z, Wang S, et al., 2024, Research on a Classification Model Based on Pathological Data Features of Gastric Tumors. *Journal of Instrumentation and Measurement*, Online ahead of print.
- [11] Wang H, Guo M, Sun Y, et al., 2024, Research and Diagnostic Value of AI-Based Cytopathology Diagnostic System for Lung Cancer. *Journal of PLA Medical College*, 45(5): 463–468.
- [12] Hou N, Zhai W, Zheng J, 2024, Micro Knowledge through Macro Vision: Application Status and Challenges of AI in Digital Pathology of Renal Cancer. *Chinese Journal of Cancer Prevention and Treatment*, 16(2): 143–151.
- [13] Fan L, Song Z, Deng L, et al., 2024, Research Progress of AI in Pathological Diagnosis and Molecular Typing of Prostate Cancer. *Journal of Naval Medical University*, 45(9): 1141–1146.
- [14] Xie Y, 2023, Application of AI in Pathological Diagnosis and Prognosis of Metastatic Lymph Nodes in Hypopharyngeal Squamous Cell Carcinoma, dissertation, Shandong University.
- [15] Zhai T, Zhang M, Li D, 2024, Research Progress of AI in Imaging Diagnosis and Treatment of Breast Cancer. *Journal of Molecular Imaging*, 47(9): 1003–1006.
- [16] Chu X, Fu Y, Zheng S, et al., 2024, Opportunities and Challenges of AI in Imaging of Primary Liver Cancer. *Radiologic Practice*, 39(9): 1244–1249.
- [17] Wu Y, Hao J, 2024, Research Progress of Radiomics in Diagnosis and Treatment of Gallbladder Cancer. *International Journal of Medical Radiology*, 47(5): 594–598.
- [18] Jia W, Wang L, 2024, Research Progress of AI in MRI of Pituitary Tumors. *Magnetic Resonance Imaging*, 15(9): 162–166.
- [19] Deng B, Huang W, Jiang Y, 2024, Advances in AI-Based Precision Diagnosis and Treatment of Lung Cancer Using CT Imaging. *Chongqing Medicine*, Online ahead of print.

Publisher's note

Bio-Byword Scientific Publishing remains neutral with regard to jurisdictional claims in published maps and institutional affiliations.